



Implementation of aerosol-cloud interactions in the regional atmosphere-aerosol model COSMO-MUSCAT and evaluation using satellite data

Sudhakar Dipu¹, Johannes Quaas¹, Ralf Wolke², Jens Stoll², Andreas Mühlbauer³, Marc Salzmann¹, Bernd Heinold², and Ina Tegen²

¹Institute for Meteorology, Universität Leipzig, Germany

²Leibniz Institute for Tropical Research, Germany

³FM Global Research, Norwood, MA, U.S.A

Correspondence to: Dipu Sudhakar (dipu.sudhakar@uni-leipzig.de)

Abstract. The regional atmospheric model Consortium for Small Scale Modeling (COSMO) coupled to the MultiScale Chemistry Aerosol Transport model (MUSCAT), is extended in this work to represent aerosol-cloud interactions. Previously, only one-way interactions (scavenging of aerosol and in-cloud chemistry) and aerosol-radiation interactions were included in this model. The new version allows for a microphysical aerosol effect on clouds. For this, we use the optional two-moment cloud microphysical scheme in COSMO and the online-computed aerosol information for cloud condensation nuclei (CCN) concentrations, replacing the constant CCN concentration profile. In the radiation scheme, we implement a droplet-size-dependent cloud optical depth, allowing now for aerosol-cloud-radiation interactions. In order to evaluate the model with satellite data, the Cloud Feedback Model Inter-comparison Project Observational Simulator Package (COSP) has been implemented. A case study has been carried out to understand the effects of the modifications, in which the modified modeling system was applied over the European domain with a horizontal resolution of $0.25^\circ \times 0.25^\circ$. It is found that the online coupled aerosol introduces significant changes for some cloud microphysical properties. The cloud effective radius shows an increase of 2 to 10 μm , and the cloud droplet number concentration is reduced by 10 to 50 cm^{-3} . For both quantities, the new model version shows a better agreement with the satellite data. The microphysics modifications have a smaller effect on other parameters such as optical depth, cloud water content, and cloud fraction.

1 Introduction

The quantification of aerosol cloud interactions in models continues to be a challenge (IPCC, 2013). Estimates of effective radiative forcing and assessments of the radiative effects due to aerosol cloud interactions to a large extent rely on numerical modeling. A large effort has been made to represent such effects in general circulation models (GCM) (Penner *et al.*, 2006; Quaas *et al.*, 2009; Ghan *et al.*, 2016). However, GCMs do not resolve the processes relevant for cloud dynamics well. Improved process understanding for aerosol-cloud interactions thus largely relies on simulations with cloud-resolving and large-eddy simulations (LES) (Ackerman *et al.*, 2000, 2004; Xue *et al.*, 2006; Sandu *et al.*, 2008; Seifert *et al.*, 2015; Berner *et*



al., 2013). However, LES often focus on case studies and use idealised boundary conditions and also an idealised representation of the aerosol. This leads to uncertainties in particular because, when analyzing cloud systems, or cloud regimes, rather than individual clouds, aerosol-cloud-precipitation interaction processes often are buffered (Stevens and Feingold, 2009). Regional climate modeling is a powerful tool to overcome these limitations of small-domain, idealised LES. Much higher resolutions are possible than for GCMs. Compared to LES that only simulate individual cloud systems, feedbacks between clouds and aspects of the large-scale circulation and its variability are simulated by regional climate models. Although regional models do not describe part of the large scale feedbacks which are included in GCMs, regional modeling allowing for an optimal compromise (Bangert et al., 2011; Van den Heever and Cotton, 2007; Chapman et al., 2009; Forkel et al., 2015; Yang et al., 2012).

Cloud microphysical processes are necessarily parameterized in any atmospheric model, since they act at scales down to μm . For cloud microphysics, different degrees of complexity are possible. A still often applied cloud microphysics parameterization in numerical weather prediction is a bulk, one-moment scheme (Kessler, 1969; Lin et al., 1983), which uses the specific mass for different hydrometeor species as prognostic variables. These models do not carry information about size or number concentration of cloud droplets, which are, however, essential for aerosol cloud interactions. In contrast, bin microphysical schemes numerically resolve the size spectrum and are thus able to predict the spatio-temporal behavior of a number of size categories for each hydrometeor explicitly (Khain et al., 2000; Simmel et al., 2015). This approach, however, is numerically very expensive especially when applied for regional atmospheric models. As a compromise between these two approaches, two-moment microphysical schemes are able to predict the number concentration of the liquid and ice hydrometeors, in addition to mass variables (Cotton et al., 1986; Meyers et al., 1997; Seifert and Beheng, 2006). Furthermore, numerous studies have shown that two-moment scheme is a promising avenue to be used in future operational forecast models (Reisner et al., 1998; Tao et al., 2003; Seifert and Beheng, 2006) and is also computationally efficient.

At present, several weather prediction and global models have applied two-moment cloud microphysical schemes. For example, the Weather Research and Forecasting model (WRF) is available with different types of two-moment microphysical schemes (Thompson et al., 2008; Morrison et al., 2008; Lim et al., 2010). Morrison et al. (2009) demonstrated the trailing stratiform precipitation in an idealized two-dimensional squall case with WRF model, which is consistent with surface observations. In another study, Li et al. (2008) investigated the effect of aerosol on cloud microphysical processes with a two-moment microphysical scheme in WRF model. Also, Lim et al. (2010) have included the prognostic equation for cloud water and cloud condensation nuclei (CCN) number concentration, which could reduce the uncertainty to investigate the aerosol effect on cloud properties and the precipitation process in WRF model. Furthermore Weverberg et al. (2014) discuss the comparison between one-moment and two-moment microphysical schemes in the Consortium for Small Scale Modeling atmospheric model (COSMO). This study emphasizes the improvement of physical processes with the two-moment scheme. Similarly, other groups previously implemented aerosol-cloud interactions in COSMO, albeit with a different aerosol scheme (Bangert et al., 2011; Zubler et al., 2011; Possner et al., 2015). Also, most of the models have implemented bulk microphysical schemes, however very few are coupled to the radiation scheme (Seifert et al., 2012).

In this paper we discuss the improved cloud microphysics parameterization in the COSMO model (Doms et al., 1999), via the online-coupled aerosol model, MUlti-Scale Chemistry-Aerosol Transport (MUSCAT; (Wolke et al., 2004, 2012)). The



two-moment cloud microphysical scheme in the COSMO model (*Seifert and Beheng, 2006*) uses fixed profiles of CCN concentrations. Rather than this simplification, here we use CCN concentrations predicted on the basis of the simulated aerosol from the MUSCAT module. This will enable the COSMO model to have temporally and spatially varying CCN concentrations at each grid point, which are fully consistent with the cloud and precipitation fields, as well as with dynamics (e.g. scavenging is taken into account, as is vertical transport) to represent aerosol cloud interactions. In two further steps, (i) the radiation scheme is slightly revised to take into account the cloud droplet size information (so far considered constant even when applying the two-moment cloud microphysical scheme), and (ii) a diagnostic tool, the Cloud Feedback Model Intercomparison Project Observational Simulator Package (*Bodas-Salcedo et al., 2011, 2008; Nam and Quaas, 2012*) is implemented that allows for a consistent evaluation using satellite observations. The paper is organized as follows; section 2 gives a brief introduction to the coupled model systems, data and methodology. The comparison between the improved two-moment cloud microphysical parameterization with the available two-moment scheme making use of the COSP satellite simulator is discussed in section 3. Finally, concluding remarks are given in section 4.

2 Data and Methodology

2.1 The COSMO-MUSCAT model and revised cloud activation

The non-hydrostatic three-dimensional model, COSMO developed for limited-area operational predictions (*Doms et al., 1999; Steppeler et al., 2003*) is used in this study. This model has been used operationally in convection permitting configurations since 2007 by the German Weather Service (Deutscher Wetterdienst, DWD) (*Baldauf et al., 2011*). In this study, we have used COSMO version 5.0, which is initialized and forced by reanalyzed data provided by the global meteorological model GME (Global Model of the Earth) of DWD, which is a hydrostatic weather prediction model (*Majewski et al., 2002*). GME operates on an icosahedral hexagonal grid having a horizontal resolution of approximately 40 km and vertical resolution of 40 layers up to 10 hPa. The COSMO model is initialized with the interpolated GME initial state and nested within GME with hourly updates of lateral boundary values. In this study, the COSMO model is configured with non convection permitting mode and uniform horizontal grid with a resolution of 0.25° (≈ 28 km). The two-moment scheme in COSMO model consists of five hydrometeors classes, namely cloud droplets, rain, ice crystals, snow and graupel. Processes considered by this scheme include the nucleation of cloud droplets, autoconversion of cloud droplets to form rain, accretion and self-collection of water droplets. The formulations have been derived by *Seifert and Beheng (2001)* from the theoretical formulation of *Beheng and Doms (1986)*. However, the radiation scheme does not yet make use of the additional information about cloud particle sizes provided by the two-moment microphysics. It uses the *Ritter and Geleyn (1992)* parameterization for the cloud optical properties in radiation scheme. According to *Ritter and Geleyn (1992)*, the cloud optical properties were approximated by the relation between specific liquid water content q_c and cloud effective radius r_e of cloud drop size distribution, thus cloud optical depth δ is expressed as,

$$\delta = \left(c_1 + \frac{c_2}{r_e} \right) q_c dz \quad (1)$$



where dz is layer thickness, and c_1 and c_2 are constants. Similarly, the effective radius r_e is related to specific cloud water content and is approximated as,

$$r_e = c_3 + c_4 q_c \quad (2)$$

where c_3 and c_4 are constants (*Ritter and Geleyn, 1992*). In order to take into account of the two-moment microphysics scheme, the simulated variable cloud droplet size, the cloud optical properties in radiation scheme have been modified. The cloud effective radius r_e is derived by dividing the third and second moment of the size distribution (*Martin et al., 1994*) which, after rearranging, yields,

$$r_e = \frac{\Gamma(\mu + 4)}{2\lambda\Gamma(\mu + 3)} \quad (3)$$

where μ is spectral shape parameter and λ is the slope parameter, which is given by

$$\lambda = \left[\frac{\pi\rho N\Gamma(\mu + 4)}{6q_c\Gamma(\mu + 1)} \right]^{\frac{1}{3}} \quad (4)$$

where ρ is the density of the air, N is the droplet number concentration, and q_c is the specific water content. The corresponding cloud optical depth is given by

$$\delta = \frac{1.5\rho q_c dz}{2\rho_w r_e} \quad (5)$$

where, dz is the layer thickness, $\rho_w = 1000 \text{ kg m}^{-3}$ the density of liquid water.

The online coupled model system COSMO-MUSCAT (*Wolke et al., 2012; Renner and Wolke, 2010; Wolke et al., 2004*) is used for prognostic cloud condensation nuclei in the cloud microphysics parameterization in COSMO model. The chemistry/aerosol transport model, MUSCAT treats atmospheric transport as well as chemical transformation, with the Regional Atmospheric Chemistry Mechanism (RACM) (*Stockwell et al., 1997*). In MUSCAT, all meteorological fields are given with respect to the uniform horizontal meteorological grid from the online coupled COSMO model, whereas the aerosol information is fed back to the COSMO model from MUSCAT. In the previous setting, the interactions only considered the radiative effects of aerosols (scattering and absorption of solar radiation), as well as the scavenging of aerosol and in-cloud aerosol chemistry. A diagram illustrating the COSMO-MUSCAT modeling set up is shown in Figure 1. In the COSMO model, the aerosol activation is without an explicit calculation of Köhler-Kelvin theory and the parameterization is based on empirical activation spectra in the form of power law relation,

$$N_{ccn} = C_{ccn} S^k, \quad S \text{ in } \% \quad (6)$$

where S is supersaturation, $C_{ccn} = 1.26 \times 10^9 \text{ m}^{-3}$, and $k = 0.308$ for continental condition or $C_{ccn} = 1.0 \times 10^8 \text{ m}^{-3}$ and $k = 0.462$ for maritime condition (*Khain et al., 2001*). Accordingly, the grid scale explicit nucleation rate is calculated from the time derivative of activation relation (*Seifert and Beheng, 2006*),

$$\left. \frac{\partial N_c}{\partial t} \right|_{nuc} = \begin{cases} C_{ccn} k S^{k-1} \frac{\partial S}{\partial z} w, & \text{if } S \geq 0, w \frac{\partial S}{\partial z} > 0, \\ & \text{and } S < S_{max}, \\ 0 & \text{else.} \end{cases} \quad (7)$$



The above parameterization scheme uses constant C_{ccn} concentrations in accordance with different atmospheric conditions. Also, S_{max} varies with atmospheric conditions (maritime C_{ccn} assumes that at $S_{max} = 1.1\%$, all C_{ccn} are already activated). As an initial step, we have used the simulated sulfate (SO_4) aerosol mass concentration information from the MUSCAT model to derive C_{ccn} concentration proxy using the following empirical relation (Boucher and Lohmann, 1995),

$$5 \quad C_{ccn} = 10^{2.21+0.41\log(mSO_4)} \quad (8)$$

where mSO_4 is the sulfate aerosol mass concentration in $\mu g m^{-3}$. The constant C_{ccn} in the equation (7) is replaced by the spatially and temporally varying C_{ccn} values, derived from equation (8), using the sulfate aerosol mass concentration from the MUSCAT module. Even though, this empirical relationship that links sulfate aerosol mass concentration to C_{ccn} are widely used is subject to substantial uncertainty. Representing sulfate aerosol as surrogate for all aerosols is probably too simple
 10 to capture the complexity of the whole activation process. Additionally, uncertainty in the Boucher and Lohmann (1995) parameterization is attributed to variations in cloud updraft velocity (Penner *et al.*, 2001).

2.1.1 Model evaluation method

The main challenges in General Circulation Models (GCM) and Numerical Weather Prediction (NWP) models are representing sub-grid scales processes in the order of few kilometers. Such processes are included by means of parameterization and
 15 satellites have been proven to be the most helpful tool for the statistical evaluation of parameterization at a large scale (eg. Lohmann *et al.* (2007); Ebert *et al.* (2007), etc.). Indeed, satellite retrievals have been used to evaluate performance of the numerous GCMs and NWP models (Quaas *et al.*, 2004, 2009; Zhang *et al.*, 2005; Brunke *et al.*, 2010; Cherian *et al.*, 2012; Nam *et al.*, 2014). A meaningful evaluation of modeling with satellite observations is challenging because of the difference in the model variables and the assumptions for the satellite retrievals. To address this problem, the integrated satellite simulator
 20 COSP (CFMIP Observational Simulator Package, Bodas-Salcedo *et al.*, 2011) has been developed within the framework of Cloud Feedback Model Intercomparison Project (CFMIP). The COSP satellite simulator produces model diagnostics, which are fully consistent to satellite products such as from the International Satellite Cloud Climatology Project (ISCCP; Rossow and Schiffer, 1999), MODerate Resolution Imaging Spectroradiometer (MODIS; Platnick *et al.*, 2003; Pincus *et al.*, 2012), Cloud-Aerosol Lidar and Infrared Pathfinder Satellite Observations (CALIPSO; Chepfer *et al.*, 2010) and the CloudSat cloud
 25 radar (Marchand *et al.*, 2009). This tool has previously been used with COSMO by Muhlbauer *et al.* (2014, 2015). The diagnostics include a variety of cloud properties, which enables consistent inter-model and model-to-observation comparisons. In the upcoming section, model simulations are mostly compared with MODIS level-2 satellite data. The satellite products are also subject to retrieval bias. In-situ validations reveal that the MODIS cloud products overestimate the in-situ measurements but are highly correlated (Noble and Hudson, 2015; Min *et al.*, 2012). The next section discusses the comparison between the
 30 different standard and new COSMO simulations and their comparison with satellite observations.



3 Results for a case study

The simulations are carried out for a time period of 10 days (15 - 25 February 2007). The weather is evidently a complex processes which exhibits lots of variations. As the forecast time progress the uncertainty in weather prediction also increases. Hence, we have considered the second day of the simulation for validating model and satellite simulators. To isolate and analyse the effects of the modifications, three different simulations were carried out, (a) COSMO two-moment (COSMO-2M), with fixed CCN, (b) COSMO two-moment with radiation coupled with microphysics (COSMO-2MR), with fixed CCN, and (c) coupled simulation, i.e. using interactive rather than prescribed CCN concentrations (COSMO-MUSCAT). In most of the discussion we have used simulations (a) and (c).

3.1 Synoptic situation

The simulation starts on 15 February and ends on 25 February 2007. The meteorological conditions at the beginning of the simulation, as well as key meteorological parameters, are illustrated in Figure 2. On February 15, the weather in Europe is dominated by a low pressure system over the north Atlantic Ocean (Figure 2a) and high pressure system over central and southern Europe. The 2-m temperature reveals a warm oceanic region (Atlantic and Mediterranean) and a cool continental European land mass, a prominent winter synoptic condition in which there is a strong temperature gradient from west to east across Europe. The oceanic region experiences a maximum temperature of 20°C , whereas the northeastern continental region experiences a minimum temperature of -20°C . The low pressure system in the Atlantic drives northerly wind with high velocity over the Atlantic Ocean, which also results in high cloud fraction over the region (Figure 2b). Further, the 500-mb wind is also strong over Mediterranean region. The cold continental air mass over Southern Europe results in cloud free regions over the Mediterranean sea and the adjoining region. However, the major part of the domain is covered with a cloud fraction close to 100%.

3.2 Evaluation with satellite data

To evaluate model simulations, the COSP satellite simulators are applied. As an initial step, the COSP-diagnosed model clouds are compared to ISCCP and MODIS cloud products. To compare with ISCCP satellite retrievals, model results are re-gridded from 28 km to 280 km resolution, using a grid interpolation method. The model derived cloud fraction is daily averaged to illustrate the comparison between model (COSP) and ISCCP satellite retrievals (Figure 3). The observed cloud fraction shows more cloud free regions compared to model simulations. The cloud free regions in the satellite observation are mainly over the Atlantic Ocean, which may be due to the poor representation of the marine stratocumulus in the low resolution satellite observation (280 km resolution). Nevertheless, it is evident that the model derived cloud fraction is in broad agreement with ISCCP satellite retrievals, allowing now for a more detailed analysis of the cloud microphysical properties that are at the center of this study. Further, flux comparison with CERES (Clouds and the Earth's Radiant Energy System) satellite products are discussed in section 3.3.



In the next step, we evaluate the model results in terms of cloud optical and microphysical properties with MODIS level-2 data sets. In the two model versions, we make use of the MODIS simulator diagnostics. The different swath data sets of MODIS level-2 on 17 February 2007 (day time overpass only) are combined and gridded to the model domain. To reduce the uncertainty in cloud phase, MODIS level-2 products and model simulations are screened for liquid phase clouds only. Figure 4 shows the comparison between MODIS observed and model simulated (day time averaged, COSP) cloud optical depth, cloud droplet effective radius, and cloud liquid water path, respectively. The top panel shows MODIS level-2 cloud products, the middle panel is COSMO-MUSCAT, and the bottom panel is the difference between COSMO-MUSCAT and COSMO-2M. In general, we find that the simulated cloud optical depth exhibits a spatial pattern similar to the observations, with a magnitude that is in agreement with MODIS level-2 retrievals (Figure 4a and d). In both cases it varies between 2 and 50, with maximum values observed over similar geographical regions. However, the satellite derived cloud optical depth and liquid water path is slightly larger in the central eastern region of the domain. Although the model derived cloud effective radius is underestimated compared to MODIS data, both exhibit a similar spatial pattern (Figure 4b and e). The model cloud droplet effective radius varies between 2 to 14 μm , whereas it is in the range between 2 to 20 μm in the satellite retrievals. The high values of satellite derived effective radius mainly are observed over the Atlantic coast, where marine stratocumulus clouds occurred. Note that MODIS possibly overestimate cloud droplet effective radius (*Min et al., 2012; Noble and Hudson, 2015*). The effect of marine stratocumulus is also visible in the case of observed MODIS cloud optical depth and cloud water path. Similar to cloud optical depth, cloud water path also exhibit comparable spatial patterns for both, model and observations. Its simulated magnitude also is in broad agreement with the satellite retrievals, with a slight underestimation in the model mainly over central eastern Europe and over the Atlantic coast. The cloud water path in both cases ranges between about 0.025 and 0.425 kg^{-3} .

The outcome of cloud microphysics modification is analyzed by considering the difference between the two simulations, which is shown in Figure 4g, h, and i. Out of the three parameters, the largest impact of the revised parameterization is found for the cloud droplet effective radius. The version considering the interactive aerosol number concentration (COSMO-MUSCAT) exhibits an increase in the cloud effective radius by a range of 2-10 μm throughout the domain, although a slight reduction can be noticed in a few areas. This indicates the impact of the activation and growth of the sulphate aerosol from MUSCAT model. In the case of cloud optical depth and cloud water path, both generally show slight increases despite of little decreases in a few places. The cloud optical depth shows a variation in the range of ± 20 and the liquid water exhibits a variation in the range of $\pm 0.16 \text{ kgm}^{-2}$. For cloud optical depth and cloud liquid water path, both model versions are equally close or distant, respectively, from the MODIS retrievals. For the cloud droplet effective radius, the revised model version (COSMO-MUSCAT) better represented the retrieved distribution.

We have also included cloud droplet number concentration N_d as a diagnostics of the model via the MODIS satellite simulator. Figures 5a, b, and c show the spatial distribution of N_d for the COSMO-2M, COSMO-MUSCAT simulations and MODIS level-2 observations. From MODIS level-2 observations, cloud droplet number concentration N_d can be expressed in terms of cloud optical depth τ_c and effective radius r_e (*Quaas et al., 2006*), which is given by,

$$N_d = \alpha \tau_c^{0.5} r_e^{-2.5} \quad (9)$$



where $\alpha = 1.37 \times 10^{-5} m^{-0.5}$. Uncertainty in derived N_d can arise from satellite droplet effective radius. As compared to COSMO-2M simulations, there is substantial reduction in the COSMO-MUSCAT derived N_d (Figure 5a and b), in which the cloud microphysics are modified. This leads to a better agreement with satellite retrievals, especially over western Europe (Figure 5d). In the basic COSMO-2M version, the cloud droplet number concentration varies between 10 to 120 cm^{-3} , whereas it is between 10 to 60 cm^{-3} in the case of coupled model simulation, which is closer to satellite retrievals, except in some regions over and to the north of the Balkans. In the basic version of the COSMO-2M, the CCN is fixed as 300 cm^{-3} , whereas the coupled model uses gridded CCN (Cloud Condensation Nuclei) information from the MUSCAT model. Figure 5c shows the vertically and daily averaged sulfate aerosol number concentration, which varies between 20 to 300 cm^{-3} . From figure 5c, the maximum aerosol mass concentration observed over south eastern Europe, on the contrary N_d shows less. This is because *Boucher and Lohmann (1995)* parameterization shows saturation of N_d over high aerosol or polluted regions (*Penner et al., 2001*). Further, it may be difficult to correlate the spatial patterns of aerosol number concentration and cloud droplet number concentration because the droplet activation also controlled by several other meteorological properties, such as vertical velocity, microphysical links.

While comparing with high resolution MODIS satellite products, the model simulation exhibits more clear grid points, which indicates that model is unable to capture the sub grid scale cloud patterns accurately (*Jason and Thomas, 2008*), which may be due to the low resolution (0.25°) of the model. Also, the COSP satellite simulator derives the cloud information using specific cloud water content, ice content and snow content from cloud microphysical scheme. Indeed, the satellite may overestimate the retrievals, however the model simulation is able to reproduce similar spatial patterns.

3.3 Aerosol-cloud-radiation interactions

In addition, we have also implemented aerosol-cloud-radiation interactions in the COSMO model, by revising the radiation scheme in order to make use of a droplet-size-dependent cloud optical depth. Incorporating aerosol-cloud-radiation interactions in the model results in a significant change in the radiation fluxes. The analysis reveals an increase in shortwave wave flux distribution, which is in the order of 10 to 40 W m^{-2} at the surface and 2 to 20 W m^{-2} at top of the atmosphere. In turn, the long wave flux distribution shows an overall reduction in the range of -2 to -20 W m^{-2} at the surface and top of the atmosphere. An exception in some increase (20 to 20 W m^{-2}) at top of the atmosphere in some regions (Figure 6). In comparison with CERES [Clouds and the Earth's Radiant Energy System, *Loeb et al. (2012)*] satellite observations, the spatial pattern and the magnitude of model simulations are comparable with satellite observations, however the differences are neither systematic nor large (Figure 7).

4 Conclusions

This paper presents an initial approach to the modification of *Seifert and Beheng (2006)* two-moment scheme in the COSMO model. This has been done with online-coupled MUSCAT model aerosol information, which allows for a microphysical aerosol effect on clouds. It has been achieved by replacing the constant cloud condensation nuclei profile in the COSMO two-moment



scheme with gridded aerosol information derived from online-coupled MUSCAT model, using the *Boucher and Lohmann* (1995) parameterization. In addition the radiation scheme was revised to a droplet-size-dependent cloud optical depth, allowing now for aerosol-cloud-radiation interactions. In order to facilitate an evaluation using satellite retrievals, the COSP satellite simulator has been incorporated into the modeling system, which runs online with the model. The model results are evaluated with satellite observations from the ISCCP, MODIS, and CERES projects and instruments, respectively. The conclusions are summarized below.

1. The modified two-moment scheme results have been compared with former version (single-moment cloud microphysics) of the COSMO model. In terms of the cloud distributions, this modification has only a minor effect.
2. A case study has been carried out to compare the model output with observations. Daily averaged cloud optical depth, droplet effective radius, and liquid water path are compared with MODIS level-2 products. The modified model simulations are in broad agreement with satellite observations. The cloud effective radius exhibits an increase and the cloud droplet number concentration shows a reduction in the modified simulation. This is due to the reduced CCN number concentrations from the MUSCAT model. The satellite retrievals suggest the revised model version is more realistic in both quantities.
3. The representation of cloud microphysical properties in the radiation scheme has been revised in order to digest the additional information about cloud particle sizes the two-moment microphysics scheme offers. Again, only minor changes in terms of the radiation budget were found. The new approach now, however, allows to explicitly take into account the radiative effects of aerosol-cloud interactions.

In next step, further improvement in two-moment scheme will be carried out through use of the newly included aerosol model M7 (*Vignati et al., 2004*) framework in the MUSCAT model, which is able to provide aerosol number concentration information to the COSMO two-moment scheme by replacing *Boucher and Lohmann* (1995) parameterization. This will make use of the more physically based cloud droplet activation parameterization used also by ?, involving different aerosol species as CCN, and thus improving the cloud droplet number calculation based.

Code and data availability

- The COSMO-MUSCAT model is freely available under public license policy. The source code, external parameters and documentation can be obtained through Ralf Wolke (wolke@tropos.de).

Acknowledgements. This work was supported by an ERC starting grant “QUAERERE” (GA no 306284). We acknowledge the development work by the COSMO consortium. We thank Axel Seifert for valuable suggestions.



References

- Ackerman, A. S., O. B. Toon, D. E. Stevens, A. J. Heymsfield, V. Ramanathan, and E. J. Welton, (2000), Reduction of tropical cloudiness by soot, *Science*, 288, 1042-1047, doi:10.1126/science.288.5468.1042.
- Ackerman, A. S., M. P. Kirkpatrick, D. E. Stevens, and O. B. Toon, (2004), The impact of humidity above stratiform clouds on indirect aerosol climate forcing, *Nature*, 432, 1014-1017, doi:10.1038/nature03174.
- Baldauf, M., A. Seifert, J. Förstner, D. Majewski, M. Raschendorfer, T. Reinhardt, (2011), Operational Convective-Scale Numerical Weather Prediction with the COSMO Model: Description and Sensitivities, *Mon. Wea. Rev.*, 139, 3887-3905.
- Bangert, M., Kottmeier, C., Vogel, B., and Vogel, H., (2011), Regional scale effects of the aerosol cloud interaction simulated with an online coupled comprehensive chemistry model, *Atmos. Chem. Phys.*, 11, 4411-4423, doi:10.5194/acp-11-4411-2011.
- Beheng, K. D., G. Doms, (1986), A general formulation of collection rates of clouds and raindrops using the kinetic equation and comparison with parameterizations, *Contrib. Atmos. Phys.* 59, 66-84.
- Berner, A. H., Bretherton, C. S., Wood, R., and Muhlbauer, A., (2013), Marine boundary layer cloud regimes and POC formation in a CRM coupled to a bulk aerosol scheme, *Atmos. Chem. Phys.*, 13, 12549-12572, doi:10.5194/acp-13-12549-2013.
- Bodas-Salcedo, A., and Coauthors, (2011), COSP: Satellite simulation software for model assessment, *Bull. Amer. Meteor. Soc.*, 92, 1023-1043.
- Bodas-Salcedo, A., M. J. Webb, M. E. Brooks, M. A. Ringer, K. D. William, S. F. Milton, and D. R. Wilson (2008), Evaluating cloud systems in the Met Office global forecast model using simulated CloudSat radar reflectivities, *J. Geophys. Res.*, 113, D00A13, doi:10.1029/2007JD009620.
- Boucher, O., and U. Lohmann, (1995), The sulfate-CCN-cloud albedo effect: A sensitivity study with two general circulation models, *Tellus*, 47 Ser. B, 281-300.
- Brunke, M. A., S. P. de Zoete, P. Zuidema, and X. Zeng, (2010), A comparison of ship and satellite measurements of cloud properties with global climate model simulations in the southeast Pacific stratus deck, *Atmos. Chem. Phys.*, 10, 6527-6536.
- Chepfer, H., S. Bony, D. Winker, G. Cesana, J. L. Dufresne, P. Minnis, C. J. Stubenrauch, and S. Zeng, (2010), The GCM Oriented CALIPSO Cloud Product (CALIPSO-GOCCP), *J. Geophys. Res.*, 115, D00H16, doi:10.1029/2009JD012251.
- Chapman, E. G. and Gustafson Jr., W. I. and Easter, R. C. and Barnard, J. C. and Ghan, S. J. and Pekour, M. S. and Fast, J. D., (2009), Coupling aerosol-cloud-radiative processes in the WRF-Chem model: Investigating the radiative impact of elevated point sources, *Atmos. Chem. Phys.*, 9, 945-964, doi:10.5194/acp-9-945-2009.
- Cherian, R., C. Venkataraman, S. Ramachandran, J. Quaas, and S. Kedia, (2012), Examination of aerosol distributions and radiative effects over the Bay of Bengal and the Arabian Sea region during ICARB using satellite data and a general circulation model, *Atmos. Chem. Phys.*, 12, 1287-1305, doi:10.5194/acp-12-1287-2012.
- Cotton, W. R., G. P. Tripoli, R. M. Rauber, E. A. Mulvihill, (1986) Numerical simulation of the effects of varying ice crystal nucleation rates and aggregation processes on orographic snowfall, *J. Clim. Appl. Meteorol.*, 25, 1658-1680.
- Doms, G. and U. Schättler, (1999), The Nonhydrostatic Limited-Area Model LM (Lokal-Modell) of DWD: Part I: *Scientific Documentation (Version LM-F90 1.35)*, Deutscher Wetterdienst, Offenbach.
- Ebert, E. Elizabeth, E. John, Janowiak, C. Kidd, (2007), Comparison of Near-Real Time Precipitation Estimates from Satellite Observations and Numerical Models, *Bull. Amer. Meteor. Soc.*, 88, 47-64.



- Forkel R., A. Balzarini, R. Baró, R. Bianconi, G. Curci, P. Jiménez-Guerrero, M. Hirtl, L. Honzak, C. Lorenz, Ulas Im, J. L. Pérez, G. Pirovano, R. S. José, P. Tuccella, J. Werhahn, R. Žabkar, (2015), Analysis of the WRF-Chem contributions to AQMEII phase2 with respect to aerosol radiative feedbacks on meteorology and pollutant distributions, *Atmos. Environ.*, *115*, 630-645, <http://dx.doi.org/10.1016/j.atmosenv.2014.10.056>.
- 5 Ghan, S., M. Wang, S. Zhang, S. Ferrachat, A. Gettelman, J. Griesfeller, Z. Kipling, U. Lohmann, H. Morrison, D. Neubauer, D. G. Partridge, P. Stier, T. Takemura, H. Wang, and K. Zhang, (2016), Challenges in constraining anthropogenic aerosol effects on cloud radiative forcing using present-day spatiotemporal variability, *Proc. Nat. Acad. Sci. USA*, doi:10.1073/pnas.1514036113.
- IPCC, Intergovernmental Panel on Climate Change (2013), *Climate change*.
- Jason, A., O., and Thomas J. Greenwald, (2008), Comparison of WRF Model-Simulated and MODIS-Derived Cloud Data, *Mon. Wea. Rev.*,
10 *136*, 1957-1970.
- Kessler, E., (1969), On the Distribution and Continuity of Water Substance in Atmospheric Circulations, *Atmos. Res.*, *38*, 109-145, doi:10.1016/0169-8095(94)00090-Z.
- Khain, A., M. Ovtchinnikov, M. Pinsky, A. Pokrovsky, H. Krugliak, (2000), Notes on the state-of-the-art numerical modeling of cloud microphysics, *Atmos. Res.*, *55*, 159 - 224.
- 15 Khain A. P., D. Rosenfeld, A. Pokrovsky, (2001), Simulating convective clouds with sustained supercooled liquid water down to 37.5 oC using a spectral microphysics model, *Geophys Res. Lett.* *28*, 3887-3890
- Li, G., Y. Wang, and R. Zhang, (2008), Implementation of a two-moment bulk microphysics scheme to the WRF model to investigate aerosol-cloud interaction, *J. Geophys. Res.*, *113*, D15211
- Lim, K. Sunny, S. Hong, (2010), Development of an Effective Double-Moment Cloud Microphysics Scheme with Prognostic Cloud
20 Condensation Nuclei (CCN) for Weather and Climate Models, *Mon. Wea. Rev.*, *138*, 1587-1612.
- Lin, Y.-L., R. D. Farley, H. Orville, (1983), Bulk parameterization of the snow field in a cloud model, *J. Clim. Appl. Meteorol.*, *22*, 1065-1092.
- Loeb, N. G., J. M. Lyman, G. C. Johnson, R. P. Allan, D. R. Doelling, T. Wong, . J. Soden, and G. L. Stephens, (2012), Observed changes in top-of-the-atmosphere radiation and upper-ocean heating consistent within uncertainty, *Nature Geosci.* *5*, 110-113, doi:10.1038/ngeo1375.
- Lohmann, U., Stier, P., Hoose, C., Ferrachat, S., Kloster, S., Roeckner, E., and Zhang, J., (2007), Cloud microphysics and aerosol indirect
25 effects in the global climate model ECHAM5-HAM, *Atmos. Chem. Phys.*, *7*, 3425-3446.
- Majewski, D., D. Liermann, P. Prohl, B. Ritter, M. Buchhold, T. Hanisch, G. Paul, W. Wergen, and J. Baumgardner, (2002) The operational global Icosahedral-Hexagonal Gridpoint Model GME: description and high-resolution tests, *J. Atmos. Sci.*, *139*, 319-338.
- Marchand, R., J. Haynes, G. G. Mace, T. Ackerman, and G. Stephens (2009), A comparison of simulated cloud radar output from the multiscale modeling framework global climate model with CloudSat cloud radar observations, *J. Geophys. Res.*, *114*, D00A20,
30 doi:10.1029/2008JD009790.
- Martin, G. M., D. W. Johnson, and A. Spice, (1994), The measurement and parameterization of effective radius of droplets in the warm stratocumulus clouds, *J. Atmos. Sci.*, *51*, 1823-1842.
- Meyers, M. P., R. L. Walko, J. Y. Harrington, W. R. Cotton, (1997), New RAMS cloud microphysics parameterization: Part II. The two-moment scheme, *Atmos. Res.* *45*, 3-39.
- 35 Min, Q., Joseph, E., Lin, Y., Min, L., Yin, B., Daum, P. H., Kleinman, L. I., Wang, J., and Lee, Y.-N., (2012), Comparison of MODIS cloud microphysical properties with in-situ measurements over the Southeast Pacific, *Atmos. Chem. Phys.*, *12*, 11261-11273, doi:10.5194/acp-12-11261-2012.



- Morrison, H., A. Gettelman, (2008), A New Two-Moment Bulk Stratiform Cloud Microphysics Scheme in the Community Atmosphere Model, Version 3 (CAM3). Part I: Description and Numerical Tests, *J. Climate*, 21, 3642-3659.
- Morrison, H., G. Thompson, V. Tatarskii, (2009), Impact of Cloud Microphysics on the Development of Trailing Stratiform Precipitation in a Simulated Squall Line: Comparison of One- and Two-Moment Schemes, *Mon. Wea. Rev.*, 137, 991-1007.
- 5 Muhlbauer, A., T. P. Ackerman, R. P. Lawson, S. Xie, and Y. Zhang (2015), Evaluation of cloud-resolving model simulations of midlatitude cirrus with ARM and A-train observations, *J. Geophys. Res. Atmos.*, 120, 6597-6618. doi: 10.1002/2014JD022570.
- Muhlbauer, A., E. Berry, J. M. Comstock, and G. G. Mace (2014), Perturbed physics ensemble simulations of cirrus on the cloud system-resolving scale, *J. Geophys. Res. Atmos.*, 119, 4709-4735, doi:10.1002/2013JD020709.
- Nam, C., J. Quaas, R. Neggers, C. Siegenthaler-Le Drian, and F. Isotta, (2014), Evaluation of boundary layer cloud parameterizations
10 in the ECHAM5 general circulation model using CALIPSO and CloudSat satellite data, *J. Adv. Model. Earth Syst.*, 6, 300-314, doi:10.1002/2013MS000277.
- Nam, C., and J. Quaas, (2012), Evaluation of clouds and precipitation in the ECHAM5 general circulation model using CALIPSO and CloudSat, *J. Clim.*, 25, 4975-4992, doi:10.1175/JCLI-D-11-00347.1.
- Noble, S. R., and J. G. Hudson (2015), MODIS comparisons with northeastern Pacific in situ stratocumulus microphysics, *J. Geophys. Res.*
15 *Atmos.*, 120, 8332-8344, doi:10.1002/2014JD022785.
- Penner, J. E., Andreae, M., Annegarn, H., Barrie, L., Feichter, J., Hegg, D., Jayaraman, Leaitch, R., Murphy, D., Nganga, J., and Pitari, G.: Aerosols, their Direct and Indirect Effects, in: Climate Change 2001: The Scientific Basis, Contribution of working group I to the Third Assessment Report of the Intergovernmental Panel on Climate Change, edited by: Houghton, J. T., Ding, Y., Griggs, D. J., Noguer, M., Van der Linden, P. J., Dai, X., Maskell, K., and Johnson, C. A., *Cambridge Univ. Press, New York*, 881.
- 20 Penner, J. E. and Quaas, J. and Storelvmo, T. and Takemura, T. and Boucher, O. and Guo, H. and Kirkevåg, A. and Kristjánsson, J. E. and Seland, Ø., (2006), Model intercomparison of indirect aerosol effects, *Atmos. Chem. Phys.*, 6, 11, 3391-3405.
- Pincus, R., S. Platnick, S. A. Ackerman, R. S. Hemler, and R. J. P. Hofmann, (2012), Reconciling simulated and observed views of clouds: MODIS, ISCCP, and the limits of instrument simulators, *J. Climate*, 25, 4699-4720. doi:10.1175/JCLI-D-11-00267.1
- Platnick, S., King, M. D., Ackerman, S. A., Menzel, W. P., Baum, B. A., Riedi, J. C., and Frey, R. A., (2003) The MODIS cloud products:
25 Algorithms and examples from Terra, *IEEE Trans. Geosci. Remot. Sens.*, 41, 459-473.
- Possner, A., Zubler, E., Lohmann, U., and Schär, C., (2015), Real-case simulations of aerosol-cloud interactions in ship tracks over the Bay of Biscay, *Atmos. Chem. Phys.*, 15, 2185-2201, doi:10.5194/acp-15-2185-2015.
- Quaas, J., Y. Ming, S. Menon, T. Takemura, M. Wang, J. Penner, A. Gettelman, U. Lohmann, N. Bellouin, O. Boucher, A. M. Sayer, G. E. Thomas, A. McComiskey, G. Feingold, C. Hoose, J. E. Kristjánsson, X. Liu, Y. Balkanski, L. J. Donner, P. A. Ginoux, P. Stier, B.
30 Grandey, J. Feichter, I. Sednev, S. E. Bauer, D. Koch, R. G. Grainger, A. Kirkevåg, T. Iversen, Ø. Seland, R. Easter, S. J. Ghan, P. J. Rasch, H. Morrison, J. -F. Lamarque, M. J. Iacono, S. Kinne, and M. Schulz, (2009), Aerosol indirect effects - general circulation model intercomparison and evaluation with satellite data, *Atmos. Chem. Phys.*, 9, 8697-8717, doi:10.5194/acp-9-8697-2009.
- Quaas, J., O. Boucher, and F. -M. Bréon, (2004), Aerosol indirect effects in POLDER satellite data and in the Laboratoire de Météorologie Dynamique-Zoom (LMDZ) general circulation model, *J. Geophys. Res.*, 109, D08205, doi:10.1029/2003JD004317.
- 35 Quaas, J., O. Boucher, and U. Lohmann, (2006), Constraining the total aerosol indirect effect in the LMDZ and ECHAM4 GCMs using MODIS satellite data, *Atmos. Chem. Phys.*, 6, 947-955, doi:10.5194/acp-6-947-2006.
- Reisner, J., R. M. Rasmussen, R. T. Bruintjes, (1998), Explicit forecasting of supercooled liquid water in winter storms using the MM5 mesoscale model, *Q. J. Royal Meteorol. Soc.* 124, 1071-1107.



- Renner, E., R. Wolke, (2010), Modelling the formation and atmospheric transport of secondary inorganic aerosols with special attention to regions with high ammonia emissions, *Atmos. Environ.*, *44*, 1904-912.
- Ritter, B., and J. Geleyn, (1992), A Comprehensive Radiation Scheme for Numerical Weather Prediction Models with Potential Applications in Climate Simulations, *Mon. Wea. Rev.*, *120*, 303-325.
- 5 Rossow, W. B., and R. A. Schiffer, (1999), Advances in understanding clouds from ISCCP, *Bull. Amer. Meteorol. Soc.*, *80*, 2261-2288, doi:10.1175/1520-0477(1999)080<2261:AIUCFI>2.0.CO;2.
- Sandu, I., J. L. Brenguier, O. Geoffroy, O. Thouron and V. Masson, (2008), Aerosols impacts on the diurnal cycle of marine stratocumulus, *J. Atmos. Sci.* *65*, 2705-2718.
- Seifert, A., T. Heus, R. Pincus, and B. Stevens (2015), Large-eddy simulation of the transient and near-equilibrium behavior of precipitating shallow convection, *J. Adv. Model. Earth Syst.*, *7*, 1918-1937, doi:10.1002/2015MS000489.
- Seifert, A., C. Köhler, and K. D. Beheng, (2012), Aerosol-cloud-precipitation effects over Germany as simulated by a convective-scale numerical weather prediction model, *Atmos. Chem. Phys.*, *12*, 709-725.
- Seifert, A. and K. D. Beheng, (2006) A two-moment cloud microphysics parameterization for mixed-phase clouds. Part I: Model description, *Meteorol. Atmos. Phys.*, *92*, 45-66.
- 15 Seifert, A. and K. D. Beheng, (2001), A double-moment parameterization for simulating autoconversion, accretion and selfcollection, *Atmos. Res.*, *59-60*, 265-281.
- Simmel, M., Bühl, J., Ansmann, A., and Tegen, I., (2015), Ice phase in altocumulus clouds over Leipzig: remote sensing observations and detailed modeling, *Atmos. Chem. Phys.*, *15*, 10453-10470, doi:10.5194/acp-15-10453-2015.
- Stappeler, J., G. Doms, U. Schüttler, H. W. Bitzer, A. Gassmann, U. Damrath, Gregoric (2003), Meso-gamma scale forecasts using the nonhydrostatic model LM, *Met. Atmos. Phys.*, *82*, 75-96.
- 20 Stevens Bjorn and Feingold Graham (2009), Untangling aerosol effects on clouds and precipitation in a buffered system, *Nature*, *7264*, 607-613.
- Stockwell, W.R., Kirchner, F., Kuhn, M., Seefeld, S., (1997), A new mechanism for regional atmospheric chemistry modeling, *J. Geophys. Res.*, *102*, (D22), 25847-25879.
- 25 Tao, W.-K., J. Simpson, D. Baker, S. Braun, M. -D. Chou, B. Ferrier, D. Johnson, A. Khain, S. Lang, B. Lynn, C. -L. Shie, D. Starr, C. -H. Sui, Y. Wang and P. Wetzell, (2003), Microphysics, radiation and surface processes in the Goddard Cumulus Ensemble (GCE) model, *A Special Issue on Non-hydrostatic Mesoscale Modeling, Meteorology and Atmospheric Physics*, *82*, 97-137.
- Thompson, Gregory, P. I. R. Field, R. M. Rasmussen, W. D. Hall, (2008), Explicit Forecasts of Winter Precipitation Using an Improved Bulk Microphysics Scheme. Part II: Implementation of a New Snow Parameterization *Mon. Wea. Rev.*, *136*, 5095-5115.
- 30 Vignati, E., J. Wilson and P. Stier, (2004), M7: An efficient size-resolved aerosol microphysics module for large-scale aerosol transport models, *J. Geophys. Res.* *109*, D22202.
- Van den Heever, Susan C. and Cotton, William R., (2007), Urban Aerosol Impacts on Downwind Convective Storms, *J. of Appl. Meteor. Climatol.*, *46*, 828-850.
- Weverberg Van, K., E. Goudenhoofd, U. Blahak, E. Brisson, M. Demuzere, P. Marbaix, J. -P. van Ypersele, (2014), Comparison of one-moment and two-moment bulk microphysics for high-resolution climate simulations of intense precipitation, *Atmos. Res.*, *147-148*, 145-161.
- 35 Wolke R., W. Schröder, R. Schrödner, E. Renner, (2012), Influence of grid resolution and meteorological forcing on simulated European air quality: a sensitivity study with the modeling system COSMO-MUSCAT, *Atmos. Environ.*, *53*, 110-130.



- 5 Wolke, R., O. Knoth, O. Hellmuth, W. Schröder and E. Renner (2004), The parallel model system LM-MUSCAT for chemistry-transport simulations: Coupling scheme, parallelization and application, in: G. R. Joubert, W. E. Nagel, F. J. Peters, and W. V. Walter, Eds., *Parallel Computing: Software Technology, Algorithms, Architectures, and Applications*, Elsevier, Amsterdam, The Netherlands, 363-370.
- Xue, H., and G. Feingold, (2006), Large eddy simulations of trade-wind cumuli: Investigation of aerosol indirect effects, *J. Atmos. Sci.*, *63*,
1605 -1622.
- Yang, Q. and Gustafson Jr., W. I. and Fast, J. D. and Wang, H. and Easter, R. C. and Wang, M. and Ghan, S. J. and Berg, L. K. and Leung,
L. R. and Morrison, H., (2012), Impact of natural and anthropogenic aerosols on stratocumulus and precipitation in the Southeast Pacific:
a regional modelling study using WRF-Chem, *Atmos. Chem. Phys.*, *11*, 8777-8796, doi:10.5194/acp-12-8777-2012.
- Zhang, M. H., et al. (2005), Comparing clouds and their seasonal variations in 10 atmospheric general circulation models with satellite
10 measurements, *J. Geophys. Res.*, *110*, D15S02, doi:10.1029/2004JD005021.
- Zubler, E. M., D. Folini, U. Lohmann, D. Lüthi, A. Mühlbauer, S. Pousse-Nottelmann, C. Schär, and M. Wild, (2011), Implementation and
evaluation of aerosol and cloud microphysics in a regional climate model, *J. Geophys. Res.*, *116*, D02211, doi:10.1029/2010JD014572.

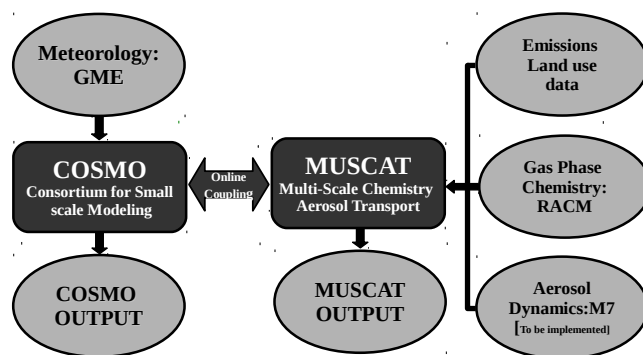


Figure 1. COSMO-MUSCAT modeling system.

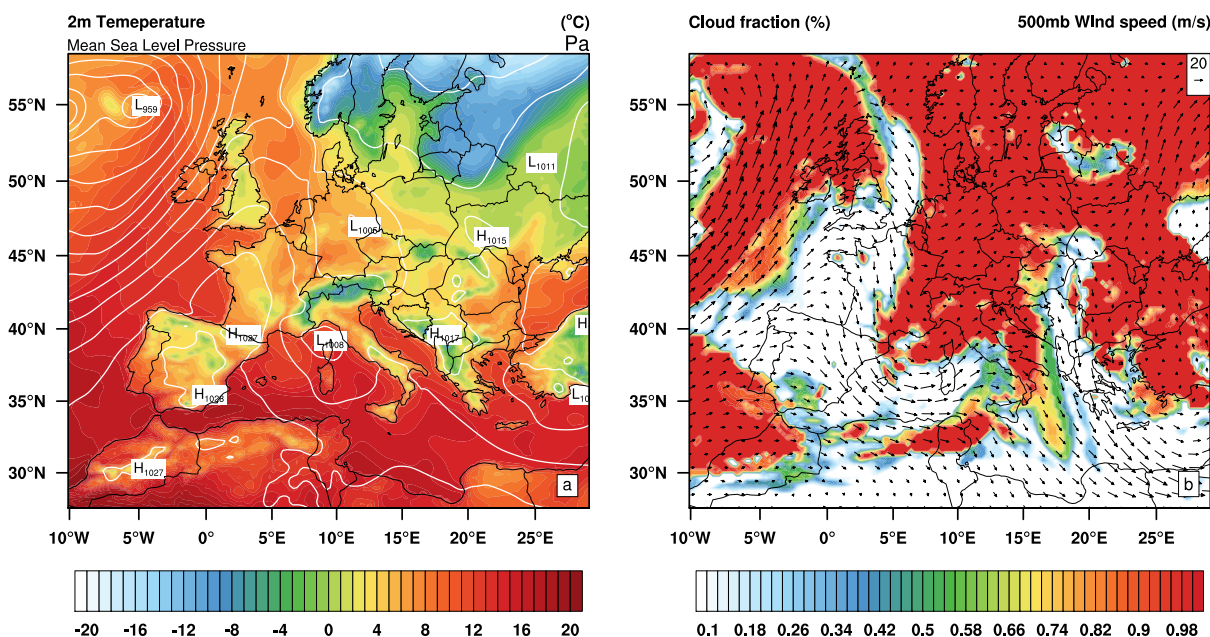


Figure 2. Synoptic conditions at the beginning of the simulation, 15 February 2007 at 00:00hrs, (a) Surface pressure in contours and 2 meter temperature in closed contours, (b) 500 mb wind vector and total cloud area fraction.

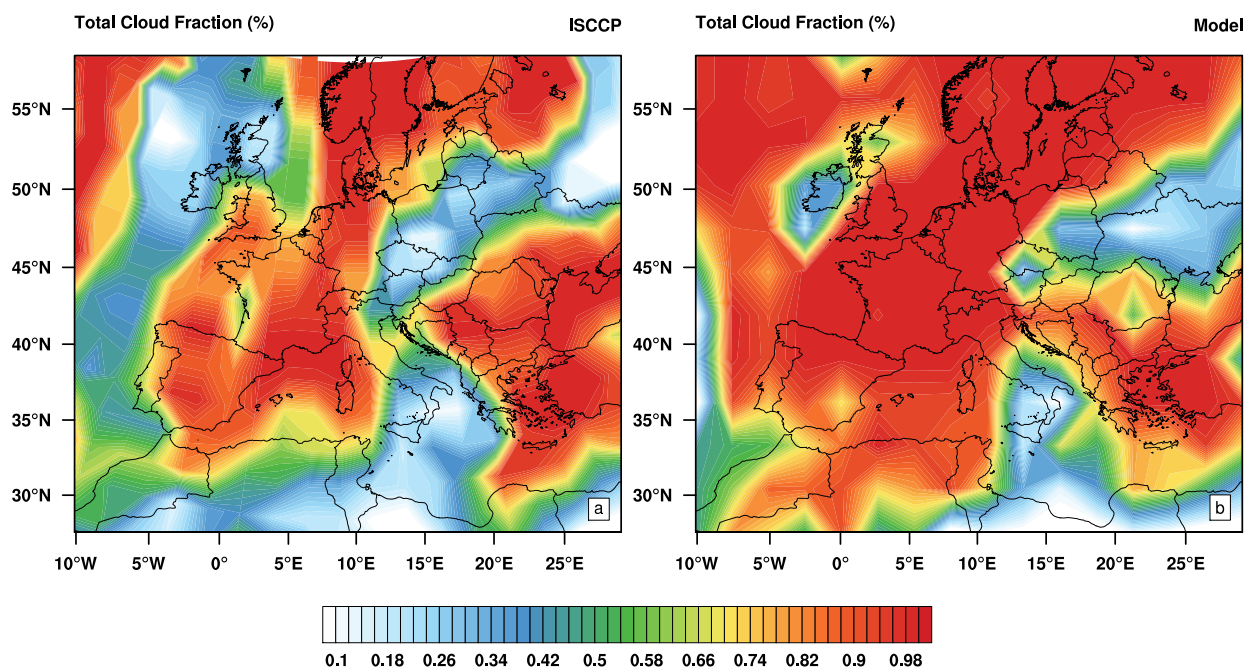


Figure 3. (a) Satellite and (b) model (COSMO-MUCAT) derived ISCCP cloud fraction, for 17 February 2007 (daily averaged).

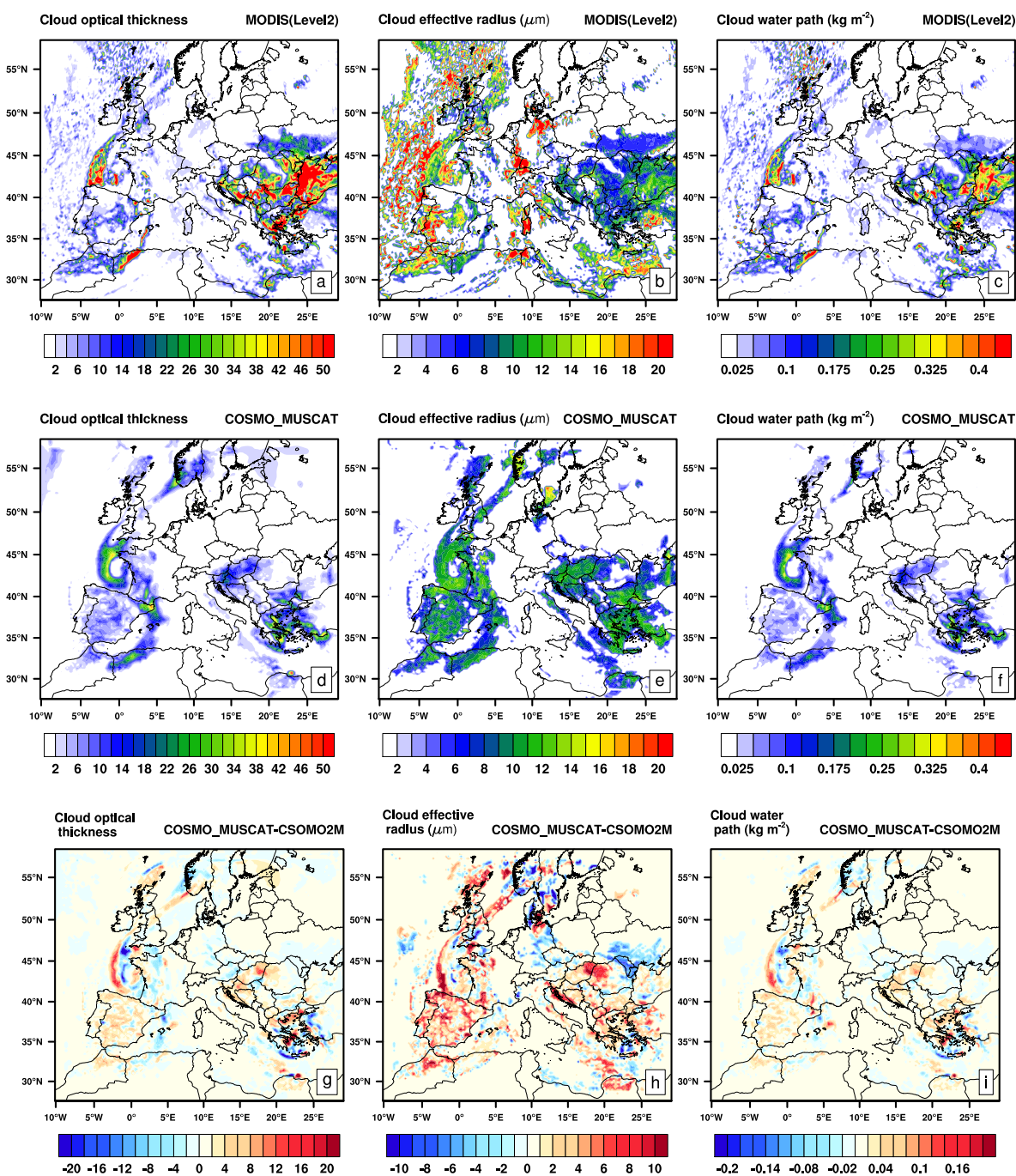


Figure 4. MODIS Level-2 (a) cloud optical depth, (b) cloud effective radius, (c) cloud water path, COSMO-MUSCAT derived (day time averaged) (d) cloud optical depth, (e) cloud effective radius, (f) cloud water path, and difference between COSMO-MUSCAT and COSMO-2M simulations(g,h,i), for 17 February 2007.

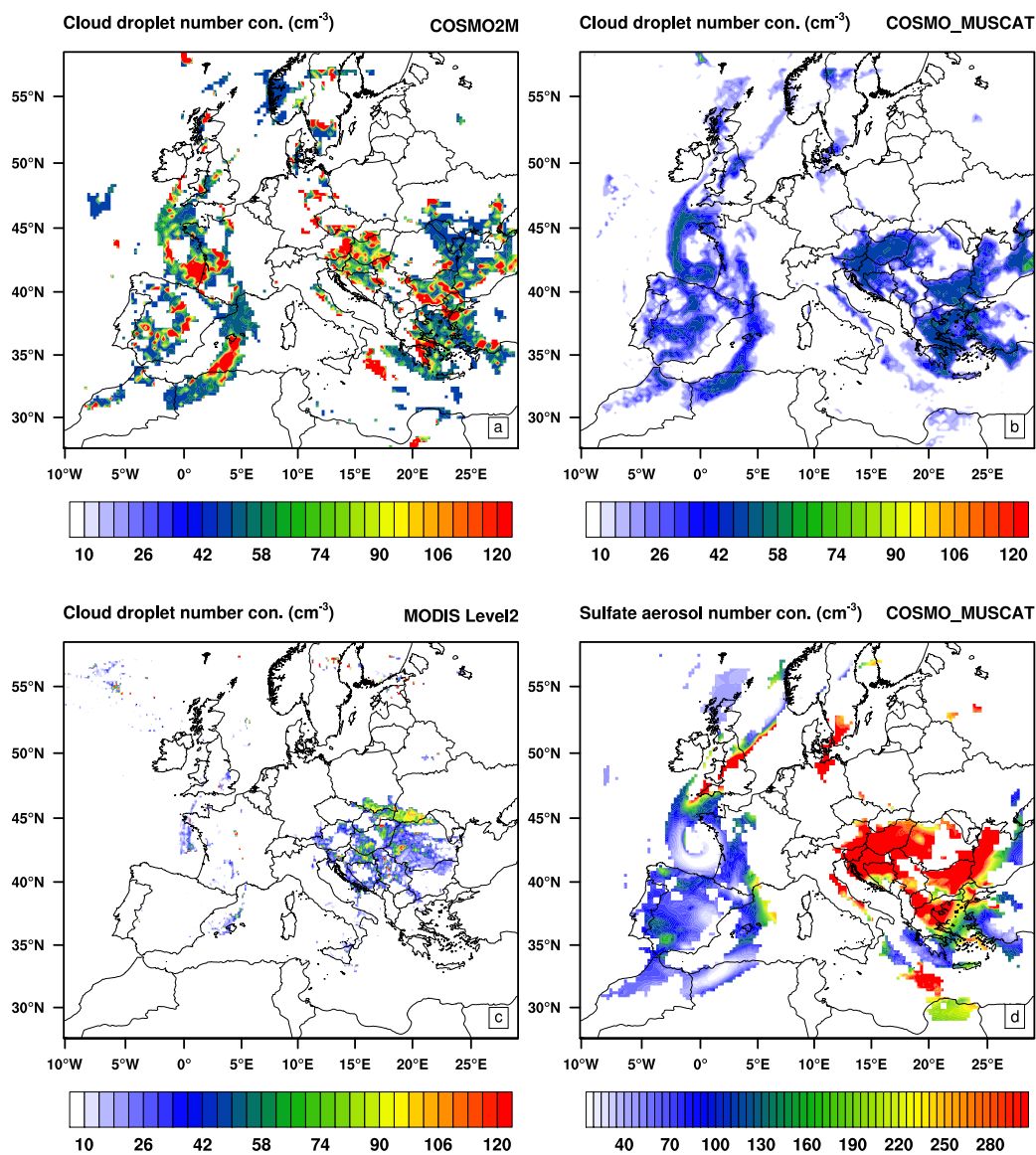


Figure 5. Day time averaged cloud droplet number concentration for (a) COSMO-2M, (b) COSMO-MUSCAT, (c)MODIS level-2 , and (d) Sulfate aerosol number concentration from MUSCAT model, for 17 February 2007.

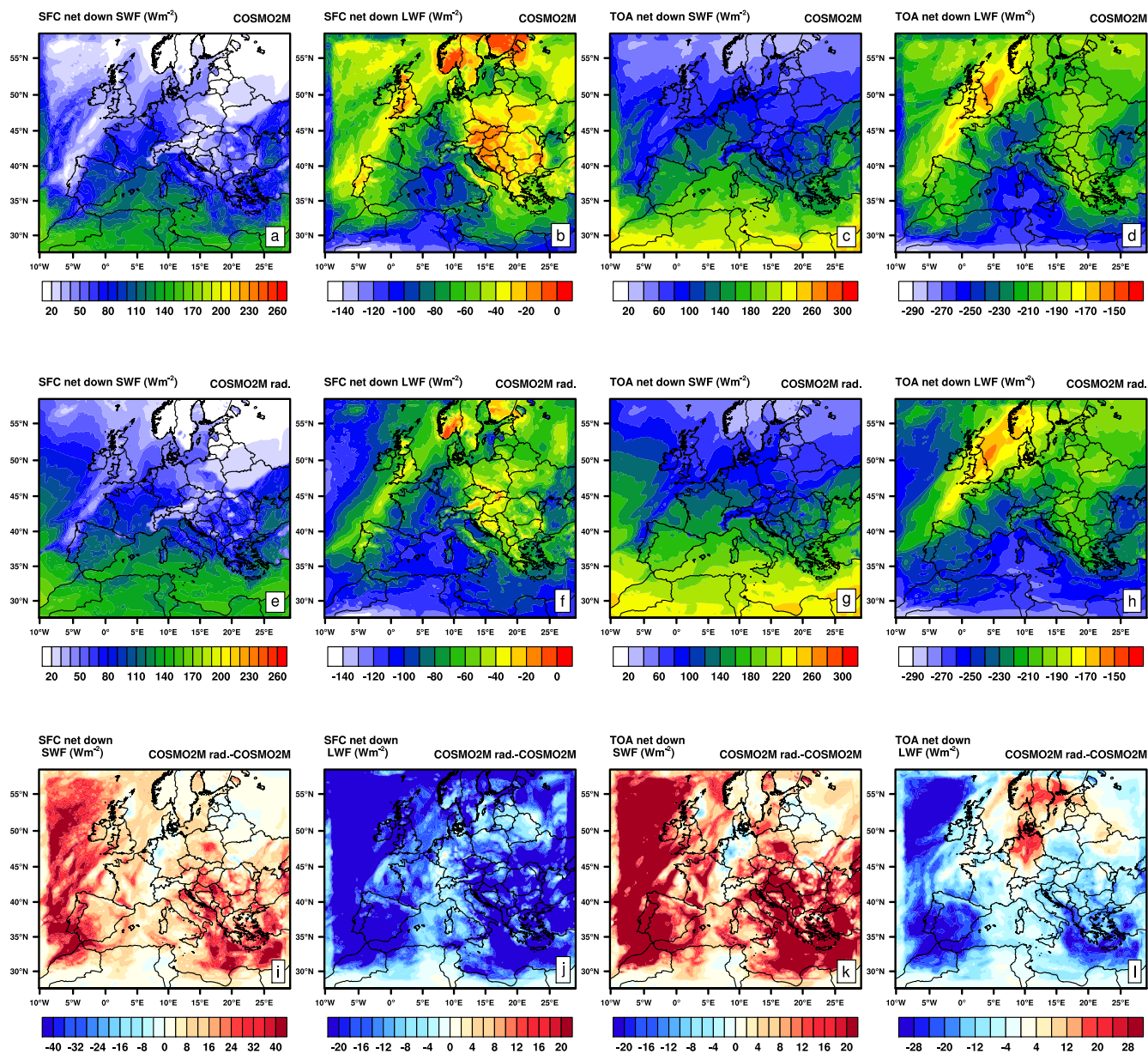


Figure 6. Comparison and difference between short wave and long wave radiation fluxes surface and top of the atmosphere, and it is difference between two simulation (COSMO-2MR radiation coupled minus COSMO-2M).

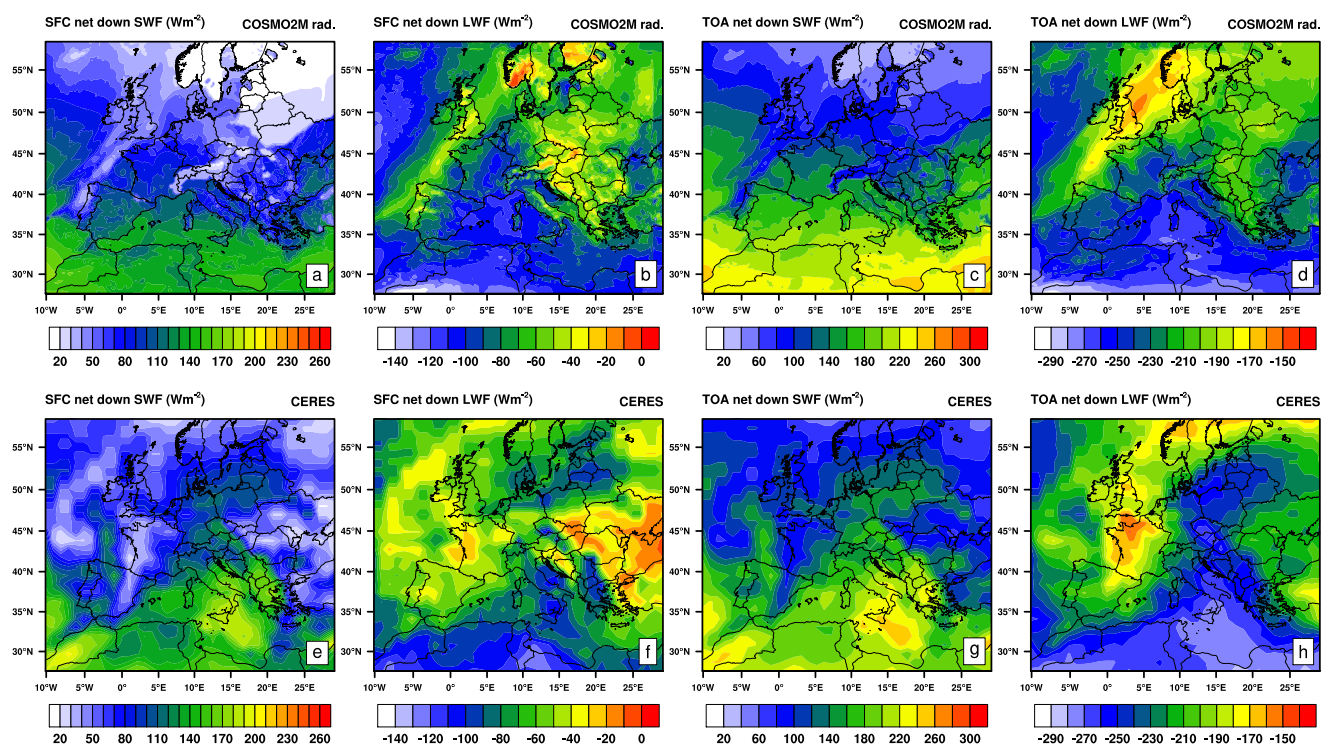


Figure 7. Comparison between short wave and long wave fluxes at surface and top of the atmosphere with CERES satellite fluxes (top panel: model COSMO-2M, bottom Panel: satellite).